USE LOCAL IMAGE CROSS-CORRELATION ON NATURAL TEXTURE TO ASSES CONCRETE DEFORMATION UNDER ITS YIELD LIMIT

Belen Ferrer [1], Julian Espinosa [2], David Mas [2*]

[1] Department of Civil Engineering, Universidad de Alicante

[2] Inst. of Physics Applied to the Sciences and Technologies, Universidad de Alicante

* Correspondence: david.mas@ua.es; Ph.: +(34) 965 903 400

ABSTRACT

Displacement of every point in a concrete specimen during some loading-unloading cycles is measured by using digital image cross-correlation (DICC) only using its original surface texture without adding or attaching any particular pattern or target to the surface. The total surface of the probe was tessellated and DICC was performed on each local area. The cross-correlation peak was refined thus obtaining improved sub-pixel correlation. In the paper, we discuss the method that was followed to select the optimal local area size and the obtained results. We show that, with natural non-optimized textures, the technique allows to locally measure the concrete deformation due to small strains (<0.1%) with an error below 50 με. Although results are more inaccurate than those obtained by a strain gauge, our method is able to non-invasively determine the strains in a concrete surface under small loads with reasonable accuracy.

KEYWORDS

Targetless tracking, local strain measurement, concrete, digital image cross-correlation, video processing, local entropy, non-invasive measurements.

1. INTRODUCTION

Image processing is a well-known discipline that has been recently introduced to structural analysis. It has evident advantages in the inspection and monitoring of buildings and structures

such as being a non-invasive technique, long distance measurement capability and wide availability since it can be implemented with not expensive devices. Considering scientific image processes that are carried out to analyze the specimens, two main different approaches are found. One of them tries to find more information from a single image while the other tries to find differences between two images of the same object that has slightly changed. This work focusses on the second one. One of the most used tool in image processing to find differences between two images is digital image correlation. This operation, which can be performed in one-dimensional signals as well as in two or even in three [1], gives the degree of similarity between two signals. Used on images (two-dimensional signal), it gives the position in which one of them (called template) best matches on the other image. In dynamics, this operation is performed between two images in order to find the movement of some pattern included in both of them.

Different modifications to this basic procedure can be implemented in order to improve its accuracy. One of these tools is the division of the whole area into several parts, allowing the calculation of correlation between each one of these parts in different states [2]. This gives an approximation to the local behavior of the material if the part is small enough. Another improvement is the interpolation of the correlation peak location in a small area around the previously found peak [3]. Besides, additional conditions can be used to allow the contour of the template to have different shapes between the initial state and the final one. This condition is called “order-shape”, with order zero meaning that no deformation is allowed between different states [4]. These features are already implemented in different specialized software like GeoPIV [5, 6], Ncorr [7] or GOMCorrelate [8] among others.

Although these applications are oriented to different fields, they share the need of a previous object preparation: specimens are covered by a pseudo-speckle (uniform random-dot) pattern in order to offer optimal conditions for obtaining digital correlation with subpixel accuracy. Therefore, the use of speckle patterns is common in tasks involving object displacements or

deformations. Usually, this pattern can be painted or projected on the surface of the object to test, which requires the material to have a uniform roughness and a non-reflective surface. With this procedure, the image is transformed to a distribution of intensities that are locally unique. The displacement of these local patterns can be measured using digital image correlation on small domains covering the whole image, thus informing about shifts or local deformations of the whole piece. The size of the spots and gradient of intensities of the textured pattern gives an idea of the goodness of the results that can be found using image correlation [4].

Concrete surfaces are also measured using this method and a speckle pattern. However, concrete is one of the most used materials in big structures (such as dams, buildings or bridges, for example) and generally the point with the largest movement is also the most inaccessible point in the structure. This fact encourages the need of measuring the concrete movement without physically reaching the point to measure, in order to avoid risk to the involved workers. Under this point of view, image techniques offer a big advantage, which unfortunately vanishes when a particular pattern needs to be painted in the surface to measure. Therefore, the measurement of concrete surface without use of any artificial pattern becomes of great interest.

Recently some studies have been made in which no additional pattern was used on the concrete surface. Alam et al. [9] used DIC together to an acoustic emission technique to measure crack opening and spacing in beams with different cross section under bending moment. Kim el al. [10] studied the influence of different threshold in the binarized images to best approach the width of cracks. Also, an extended digital image correlation which includes a distance transform algorithm was proposed by [11] to detect microcracks in targetless concrete surfaces. However, since these works are related with the appearance of cracks, strains are the highest possible in concrete and displacements will be at least those related with that maximum strains. When crack is already developed, much higher displacement will happen, hence making easier the

displacement detection. Up to our knowledge, there are few works that analyze concrete deformation when small loads are applied [12].

The use of the naked concrete surface to measure movements and deformations under its yield limit relays in the degree of similarity of this pattern with the speckle pattern successfully used until now. The particular surface texture of concrete due to its fabrication could give a good approximation to a speckle pattern. During the formwork of concrete, a good vibration must be done into the fresh concrete in order to remove all bubbles of air that were enclosed during the concrete pouring. Even with a very good vibration technique and experience, it is usual that some small bubbles stay in the walls of the formwork. When enduring, these bubbles become in small hollows in the concrete surface that can be randomly distributed or not. Additionally, changes in water, sand and gravel distributions or even external temperature during the concrete hardening make the surface to have non-uniformities that, together with the small hollows, makes a nearly random spot distribution in the surface.

Finally, and bearing in mind that our goal is to determine the real accuracy of the proposal when applied to real structures, another problem to face is uneven illumination of the region under study. Lab experiments can be designed to have optimal illumination and contrast on the image, thus helping to improve the efficiency of image processing methods. Unfortunately, on site (and in non-reachable points) light cannot be controlled and different shadows and contrast will appear in the image.

In this paper we want to take a further step on this issue by studying the real accuracy of image processing methods by using natural (non-optimal) illumination and measuring strain displacements within the compressive yield point.

The experiment is performed in a laboratory, where the compressive forces applied to the specimen can be easily controlled. Despite of this, the remaining conditions of the experiment will not optimized, so the surface of the concrete will remain naked, without any particular

pattern applied on it and the illumination on the specimen will come from the lab windows thus no artificial illumination is used to cancel the shadows on the surface.

The manuscript is detailed as follows. First, we will introduce the main methods used and the image preprocessing techniques that have been implemented in order to optimize the results. Then, in the following sections, the main results obtained are presented and discussed. The conclusions of our proposal are summarized in the last section.

2. METHODS

As we said in the introduction, the goal of this communication is to find local deformations in a concrete piece under compression tests. In this section, the image processing technique together with the implemented experiment used to find the local displacement of the image in a video sequence are detailed.

2.1 Experimental setup

A cubic concrete piece with side length of 15 cm (see Figure 1) was tested in a compression testing machine Servosis MES-350 with a limit force 3500 kN. In order to maintain its accuracy and functionality the test machine is recalibrated every year. It has two plates to apply the compression between them. On working, the machine raises the lower plate using a hydraulic actuator while the upper plate remains still. The lower plate is completely fixed in horizontal position, while the upper plate is pinned in the three dimensions to have homogeneous compression on the specimen in the case their upper and lower surfaces are not parallel.

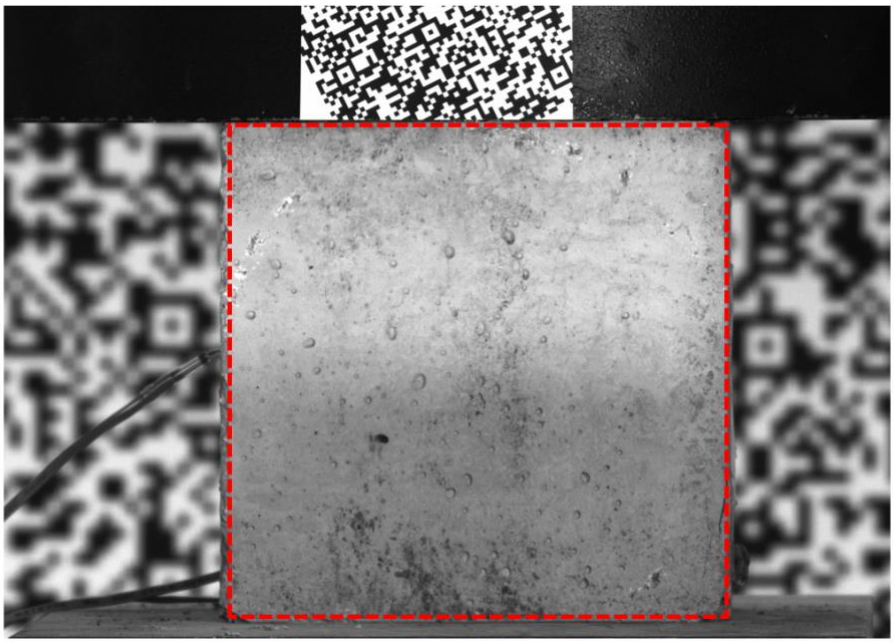

***Fig.1**: Concrete specimen located at testing machine. Red dotted line delimits the area that will be analyzed. Patterns attached to the upper part of the compression machine and in the background are set for control purposes.*

Four loading-unloading cycles were applied with a maximum load below the concrete yield limit. Using a set of 3 concrete cubes, the average failure strength of this concrete sample was set in 600 kN, so an upper limit of 400 kN was stablished as the maximum load to be reached during the experiments. The speed in both loading and unloading cycles was 5 kN/s. Some strain gauges were attached to the concrete probe, in order to check the results given by our image processing technique. Maximum strain measured through longitudinal gauge was 1000 με, which confirms that the concrete was working in elastic range during the whole experiment.

The images were recorded with a Basler camera acA640-120gc with an objective lens SIGMA 150-500 mm attached to the camera through a C-mount adapter. From the three color channels provided, from now on, we will only consider the image coming from the green channel. The camera was working with a temporal resolution of 1 frame per second and a frame size of 4600x3288 px. Due the slow speed of the loading cycles, not more than 1 frame per second was needed. Since no protecting screen was used to isolate the concrete piece, the camera was set

at a security distance, far enough to avoid debris thrown from the specimen in the case of fracture and also shadows on the sample. According to the lab limitations, this distance was 5 m from the specimen, which, with the proper objective lens provided a spatial resolution of 17.6 px/mm. A structured pattern was attached to the upper plate of the concrete testing machine (due to its uniformity) to check the relative movement of concrete with respect to the machine (Figure 1). Notice that no pattern was added or painted on the concrete surface, so all calculations were done with its natural texture. The scene was illuminated only with sunlight coming from the windows and no additional lamp was used to illuminate the concrete surface. Because of this, a clear shadow can be seen dividing the upper and the lower part of the concrete surface in Figure 1. Non-perfect illumination of the scene, despite increasing the error in the measurement, gives a better approximation to real conditions of structures in its final emplacement.

Finally, once the image system was set in place and adjusted, a sequence was taken with the machine stopped, in order to have some additional information about the calculation noise introduced by the procedure.

2.2 Image processing algorithms

In brief, the procedure followed consists of dividing the whole region of interest into some small rectangular regions, whose size was previously calculated. By analyzing the movement of the texture within these local areas, we obtain the local deformation of the concrete cube. To do so, a normalized cross correlation was calculated for each one of these regions, using the first image as reference for each one of them. In order to increase the accuracy a smooth surface was fitted to each local correlation and the peak location was refined. This allows to find the peak of the correlation with a subpixel accuracy [3].

The size of the local area is important in order to determine the degree of spatial accuracy of the method. Since the accuracy of the correlation depends on the amount of information

contained in the image, a non-optimal division will result in a less accurate method. On one hand, too small areas will provide accurate localized information, but the number of local regions needed to cover the whole area will be very high and so will be the requirements of computational time and memory. Additionally, since the texture is not homogenously distributed over the surface, a excessively small region may contain very few information. On the other hand, selection of large areas will result in efficient methods and areas with relevant information but at the cost of losing spatial accuracy in the determination of displacements. Up to our knowledge, area tessellation must be done attending to the particular texture of the concrete surface in a way that all the information of the local areas is similar, or at least, differences among them are minimum.

The Shannon's entropy is a mathematical function that is commonly used in image compression to assess the effective amount of information that is carried by a signal or an image [13]. The entropy of a gray-scale image is defined as:

$$H = -\sum_{k} p_k \log_2(p_k) \tag{1}$$

Where k is the number of gray levels and p_k is the probability associated with the gray level k, which can be estimated through the image histogram. This function measures the number of bits that are needed to codify an image, or a part of it. In our case we have used it for testing the homogeneity of the local regions in which the total image is divided.

We have implemented the following procedure. The image within the red area in Fig.1. was subdivided into a grids of size NxN, with N ranging from 5 to 100 (see the example in Fig. 2), and the entropy within each local area was evaluated. Then the mean and standard deviation of all the entropy values obtained for each grid division was calculated, thus obtaining a measure of the information dispersion.

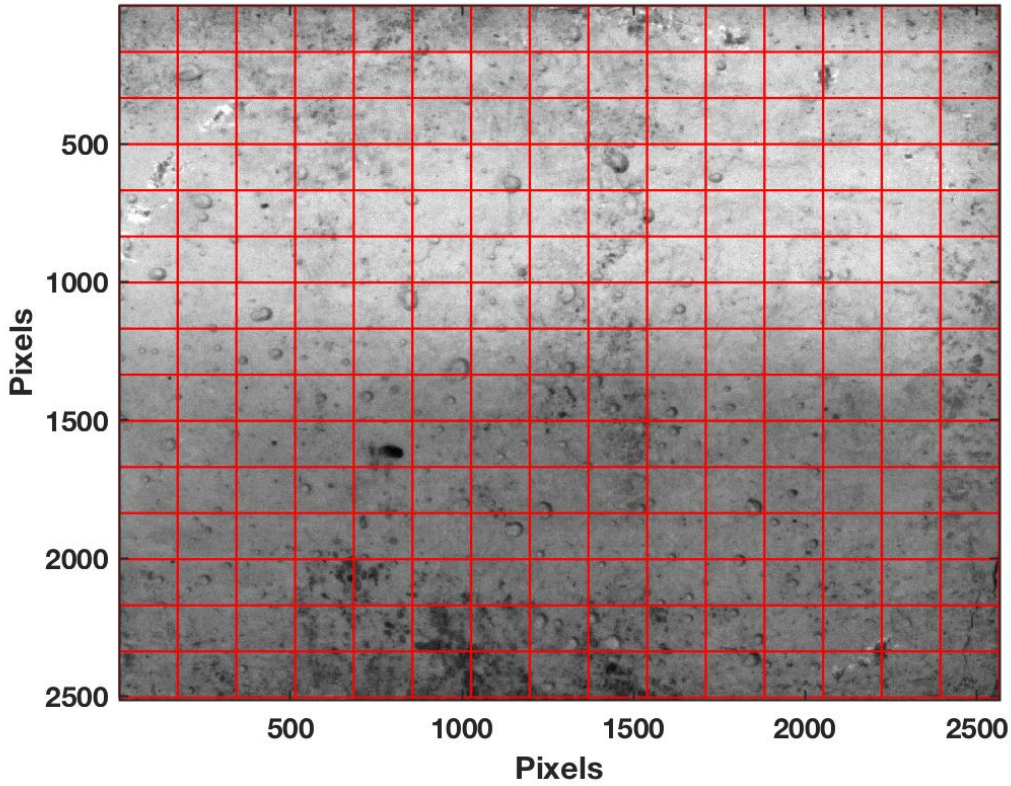

***Fig. 2**: Local regions considered on the concrete surface for local tracking of the texture elements through correlation.*

In Figure 3, we have represented the relative dispersion as the standard deviation divided by the mean value of the local areas, calculated for the different grid divisions. One can see there that there is a minimum dispersion for a 15x15 division or, equivalently, for divisions every 1 cm. According to this result, we tessellated the concrete surface in 15x15 rectangles, each one of 167x171 px. According to the resolution of the image, the local element size is of 9.49x9.72 mm.

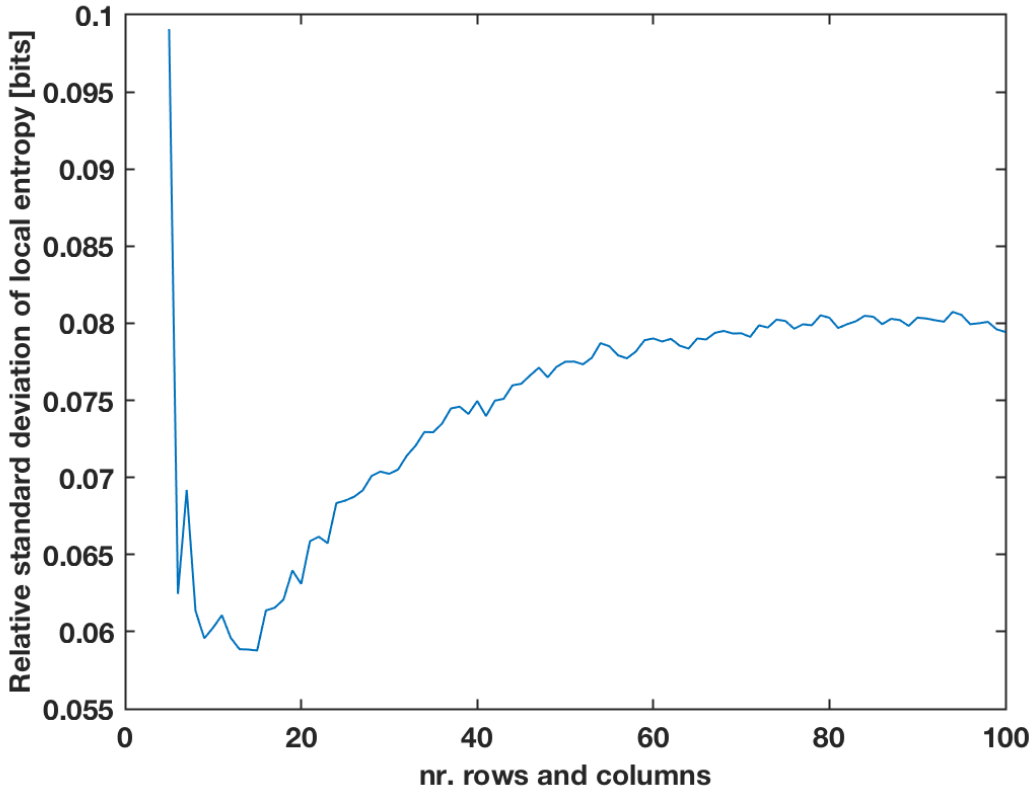

***Fig. 3**: Relative standard deviation of the local entropy in function of the grid size. The minimum reveals the grid size where the information distribution is more homogeneous.*

After determining the optimal local element size, the whole sequence, was analyzed. To this end, we consider the image from the green channel, which was codified in 8 bits, instead of binarized versions of the image. Once the concrete surface was divided into mosaic elements, a normalized cross-correlation was performed for each frame and for each local area, using the first frame as the reference image for all of them.

The obtained correlation matrix was fitted to a smooth surface following thin-plate splines [14]. To this end, only a neighborhood of 5x5 px around the correlation peak was used, and the result was an enhanced location of the peak with an accuracy of the order of 0.01 px or higher. Despite the accurate results, it is known that interpolation of the correlation surface introduces a bias in

the location of the peak. This phenomenon is called “peak-locking” and depends both of the object and the interpolation method [4]. According to the literature and to our own tests, interpolation with splines provide more accurate results than other methods [15] so we used this method here. With this interpolation, subpixel resolution in the object location was achieved

4. RESULTS

4.1. Accuracy of the method

Prior to the real measurement, the error of the procedure was calculated both theoretically and experimentally. The theoretical model provides a fast result that allow a rough estimation about the expected accuracy. On the contrary, the experimental procedure is more realistic since it evaluates the whole experimental setup but is time consuming. Here, for the sake of completeness, we explain both of them.

According to [16] the accuracy of an image-based tracking method is mainly determined by the dynamic range of the image. Being this true, one must also consider that the image is not always captured in optimal condition of illumination, contrast, etc. and thus not all available levels (or bits) are used. Therefore, the effective dynamic range that we can find in a natural image tends to be much lower. As we said above, measure of the effective amount of information that is carried in a signal is obtained through the Shannon’s entropy [13]. The entropy of an image gives an estimation of the number of bits that are required to store the image or, equivalently, the effective dynamic range used by the image. A gray-scale where all the levels are equally used presents a maximum entropy of 8. This is the case that would happen for a perfect speckle texture. On the contrary, an equally distributed black-and-white image has an entropy value of 1. Notice that this is a statistical value and does not represent the quality of the information that is contained in the image.

In the case we are dealing with, we have calculated the entropy in each of the local areas in which the image was divided (see Figure 4). Results provided an average entropy estimation of 5.67±0.38 (mean ± standard deviation) distributed as it is shown in Figure 4. This result means that only 51 ($2^{5.67}$) from 256 levels are being used. This seems reasonable, since the background is grey, and the darkest parts are not completely black, thus many levels remain unoccupied. Notice that, since these levels are lost from the beginning, image processing operations may improve the final appearance of the image, but not the total amount of information that is contained in the image.

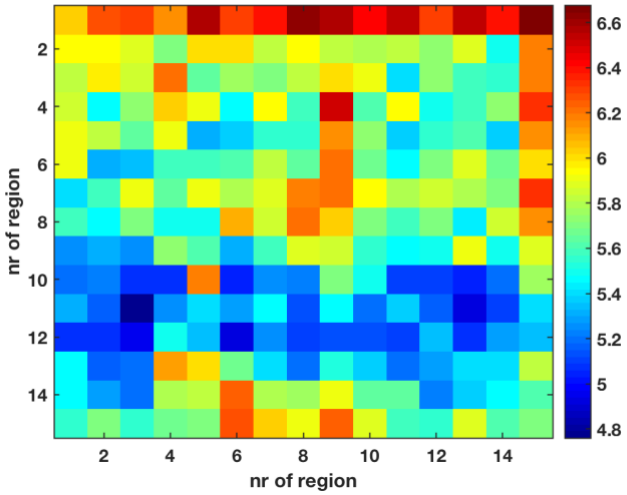

***Fig. 4**: Local entropy map calculated for each local region defined on the concrete surface according to Fig. 2*

According to [16], the maximum expected accuracy can be roughly calculated as $1/2^n$, being n the number of bits of the image codification. Therefore, and identifying the entropy as the effective number of bits, the maximum subpixel accuracy that is expected with this image can be established in 0.02 px.

In order to confirm this result and include in the accuracy calculations environmental variables like the tripod, the camera or the lens, we implemented our method on a static sequence. Since the object remains unaltered, the mean displacement measured should be zero and the

standard deviation sets the fluctuation of our measurements or equivalently, the average subpixel accuracy that can be expected. Notice that this procedure does not only take into account the calculation errors, but also the ambient noise such as vibrations or shadows together with possible drifts of the camera.

Therefore, once the concrete probe was set into the compression machine without any compression on it, the image system was set in its position and the image adjusted and focused, a video with the specimen with the machine completely stopped was taken. Using these images, the ROI and tessellate shown in figure 2 were taken to check the zero error and the maximum expected accuracy. In this case, we obtained an error of 0.01±0.03 px for the vertical position and -0.00±0.03 px for the horizontal one (see figure 5). According to this, the experimental accuracy of the method can be set in 0.03 px, which is of the same order of magnitude than the value obtained through the entropy.

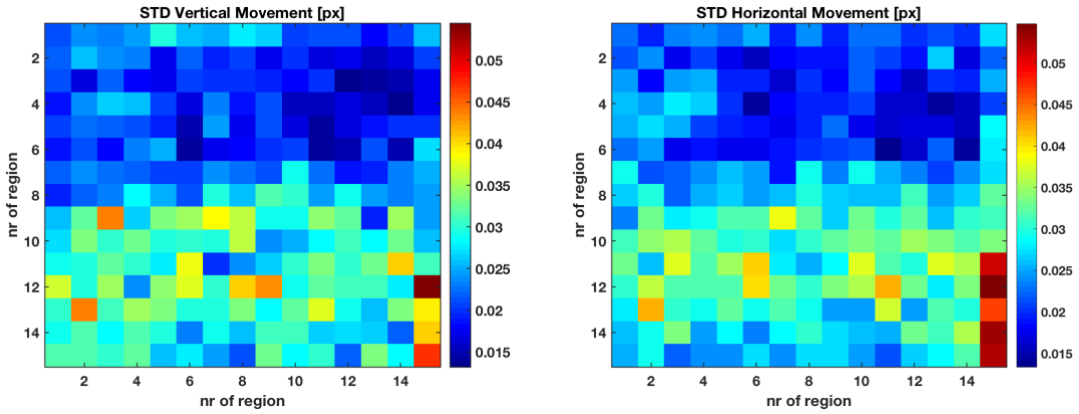

Fig. 5*: Standard error maps calculated from local tracking a static concrete cube sequence. Results are shown for both vertical and horizontal displacements*

We would like to underline that with both methods, i.e. entropy and static image, the expected accuracy of the lower part of the concrete sample is always lower than the upper part. According to Figure 2, one can see that this part corresponds to an area in the shadow. Therefore, we show here the importance of a good illumination of the specimen, and also how real measurements

in open air can have their accuracy diminished just because uneven illumination, despite the accuracy of the quality of the imaging system being used.

Summarizing these results, we can conclude that the expected experimental accuracy of our method is 0.03 px within an area of 167x171 px. or equivalently, 1.7 μm in an area of approximately 9.5x9.5 mm^2.

4.2. Testing the concrete surface

After accuracy determination of the method, the concrete piece was subjected to several load-unload cycles and the displacement in each local area has been measured. Since we are observing compression and dilation of the piece, all displacements are relative, so an internal reference has been taken. In the case of vertical compression or dilations, all movements are referred to the lower row. For horizontal movements, the reference has been the central column, i.e. column 8 of 15.

In figure 6, we show the vertical movement registered for each row averaged for all rows at the same height. In Figure 6a we depict the obtained values while Figure 6b, we depict a color map representing the vertical displacement of each column in time. The image coordinates are set so that the origin of distances is in the last row (lower part of the picture) and positive direction pointing upwards. Therefore, negative values mean that the element is approaching to the origin, which in this case represents a compression of the cube. We said above that the results from the lower part of the image have higher errors than the upper ones due to uneven illumination, but in spite of that, we decided to set the origin in the lower row. The reason is that the moving plate was located in the lower part of the concrete, while the upper part pushed against a pinned plate, so the pressure may not be uniform. Therefore, and in our opinion, the lower part was a more stable reference. Additionally, since we are representing averaged values, the noise is partially canceled, and the results are not very much affected.

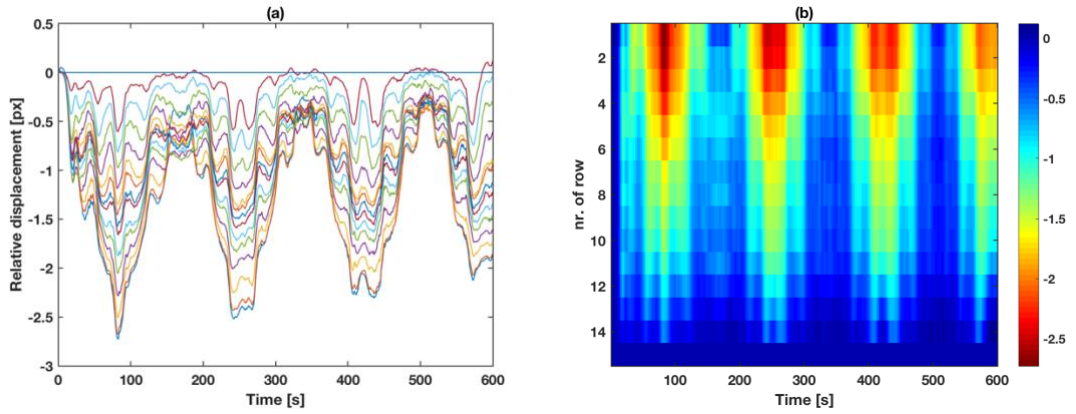

***Fig. 6**:* (a) Plot of the relative vertical displacement of each averaged row of local areas shown in figure 2. Peaks correspond to the load-unload cycles. (b) Color-coded map of the relative vertical displacement separated for each row.

In Figure 7 we represent similar plots but for the horizontal movements, which represent the expansion due to the Poisson effect. In this case, the refence for distances is set in the middle column of the image, being the positive axis pointing to the right. Therefore, negative increments in the left of the image means that the concrete piece is expanding in that direction, while positive increment in the right side means that the piece is expanding towards that direction. In fact, as expected, the piece is expanding in both directions when the compression increases and coming back to the original size when the compression is released.

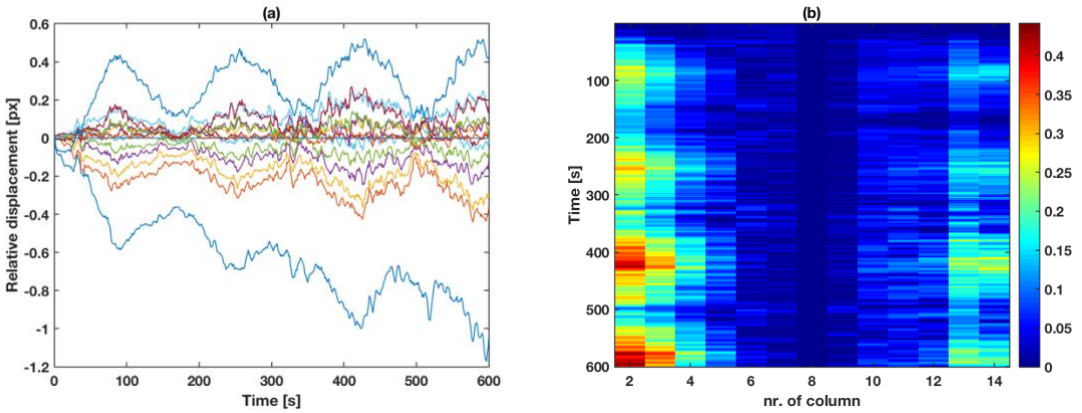

***Fig. 7**:* (a) Plot of the relative horizontal displacement of each averaged column of local areas shown in figure 2. Peaks correspond to the load-unload cycles. (b) Color-coded map of the

relative horizontal displacement separated for each column (the first and last columns have been removed to improve visualization)

We would like to point here that the first column, depicted as the blue line with a decreasing trend in figure 7(a) showed an odd behavior during the process. Also, the last column presents a displacement which seems to be larger than it should, but the case is not as evident as the previous one. Since this behavior is limited to the first and last columns and does not seem to affect to the other columns, our hypothesis is that it may be due to border effects or to small cracks close to the concrete surface due to the shrinkage during the hardening process. In order to facilitate the visualization and interpretation of the results, in figure 7(b) we have represented the displacements in absolute value without these two columns. There, we can clearly see the effect of the loading-unloading cycles in the Poisson expansion of the concrete piece.

Notice that results of displacements represented here clearly shows the subpixel nature of the method. In the case of vertical deformations, registered displacement is between 0 and 2.5 px while in the horizontal case, it hardly reaches 0.5 px, with a smooth variation during the cycles.

We would like also to underline that the exact shape of the displacement cycles depends on the size of the local region. The larger is the region, the softer and smoother are the curves although the oscillation range remains the same.

5. DISCUSSION

In the results just shown, we presented the local displacements measured for a concrete cube under progressive loads. Although results are satisfying and show that the compression and the expansion suffered by the material under small applied loads can be determined from its natural texture, it is also true that, in order to validate the method, results must be compared with other methods in the literature. Traditionally, material deformation is not measured in terms of

absolute displacements but in relative deformations or strains. The local strain for local area, i, at a time, t, can be calculated from its position according to:

$$\varepsilon_i(t) = \frac{l_i(t) - l_i(t_0)}{l_i(t_0)} \quad (2)$$

being l_i the position of the center of the local area with respect to the reference row (or column). Therefore, our results must be transformed in order to obtain comparable results. As we did in the previous section for displacements, the first step now consists of determining the error of our procedure in order to measure the strain. To do so, we have converted the results obtained for the static sequence into microstrains. In figure 8, we represent the standard deviations of strains from the static sequence obtained for rows and columns, which are connected with vertical and horizontal displacements respectively. Equivalently to the case explained above, the expected strain is 0, so the error will be determined by the standard deviation. According to the values obtained, the error of our procedure can be stablished in 20 με. This result coincides with that provided in [12] for a similar method, with comparable loads, but using a typical speckle texture instead of the natural texture of the material.

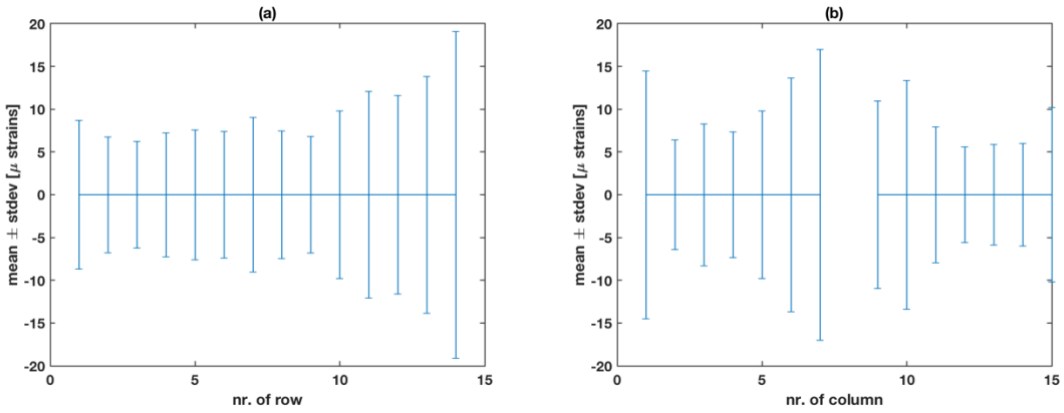

***Fig. 8**:* (a) Error-bar plot of the strain dispersion for a static sequence in the vertical direction. (b) Error-bar plot of the strain dispersion for a static sequence in the horizontal direction.

Regarding the experiment itself, in the following figures we show the deformation results. In figure 9, we depict the strains map in function of time for both vertical and horizontal directions. They correspond to the displacement fields represented in figures 6(b) and 7(b). One can see there that, contrary to what should be expected (vertical and horizontal uniform bands for 9(a) and 9(b), respectively), the camera registered different strain values for different locations in the concrete piece. This may happen because of two main reasons: the first one may be due to the border effects, which was commented before. The second reason is an effect of measure composition and error propagation. For those locations closer to the origin of distances, the error will be higher, due small distances to the reference point. This happens to lower part of the surface in vertical direction. For horizontal direction the main error is at the center, where displacements are small and also distance to the reference point; that makes almost imperceptible the horizontal strains in this area.

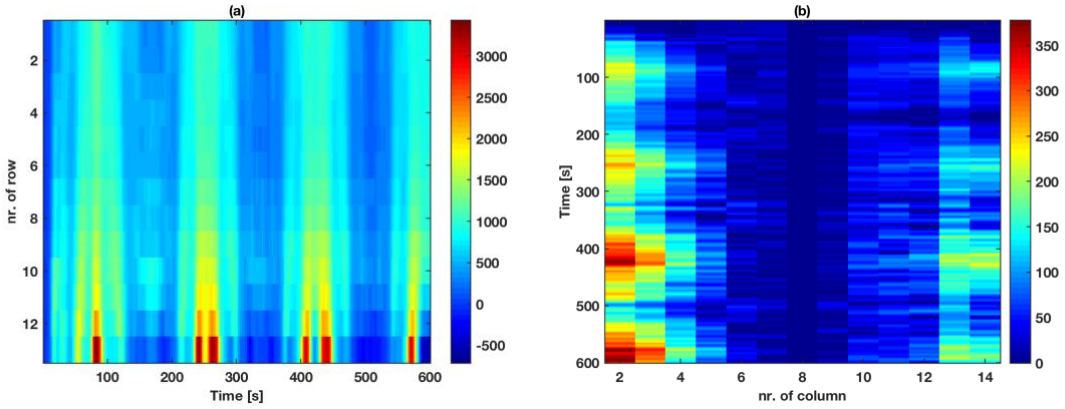

Fig. 9: (a) Strain map obtained for the vertical direction (b) Strain map obtained for the horizontal direction

In order to compare our results with those given by traditional devices, we have compared the strain results obtained with the camera with those measured with a strain gauge. In figure 10, we present the values obtained for the gauge together with those from the camera. In order to cancel out some noise from the procedure, avoid border effects and have a measurement closer

to that given by de gauges (with a length of 10 cm), in the vertical case (Figure 10(a)) we have obtained and represented the average value for the rows 3 to 13. In the horizontal case, depicted in figure 10(b), we have represented the mean value of the columns 3 and 13, thus avoiding the borders and the central region, which may produce higher errors.

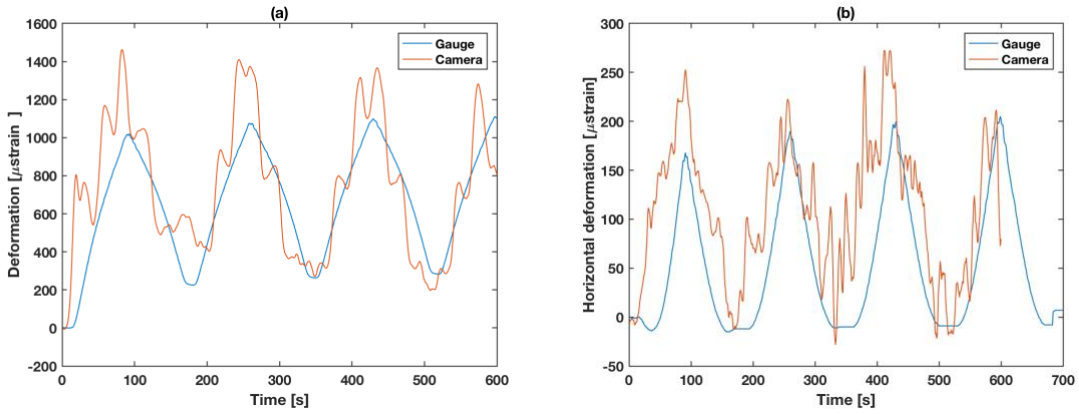

***Fig. 10**:* (a) Comparison among strain values obtained with a gauge band and the method here proposed in the vertical direction. (b) Comparison among strain values obtained with a gauge band and the method here proposed in the horizontal direction.

In Figures 9 and 10, one can see that the first cycle presents larger errors than the remaining three-ones, which can be appreciated in the first compressive stage. This may be due to small rotations of the concrete piece in the compression device due to adjustment to the plates, that remain invisible for the gauges. Counting from the first unload valley (*t=180 s*), we have determined that the mean errors obtained with our method is of *31±183* με and *51±51* με for the vertical and horizontal cases, respectively. These values are a bit higher than those obtained in [12] using a similar method. Nevertheless, we would like to recall that our texture and illumination was not optimized, so we consider that these differences are reasonable

6. CONCLUSIONS

Our aim in this paper was to demonstrate the possibility of measuring concrete displacements due to loading and unloading processes in natural conditions, i.e. without attaching or painting

a target or a particular texture and with natural illumination, which may imply non optimal contrast and uneven illumination. The test has been carried out in a laboratory, where the texture of a concrete cube surface was analyzed in order to obtain the changes due to applied load and unload cycles.

With a digital camera and using local cross correlation, we have first determined both theoretically and experimentally the expected accuracy of the method, which has been established in 0.03 px or, equivalently, 1.7 μm.

The approach to the local displacement was done by dividing the whole region of interest into small rectangular areas and finding the movement of each one of these areas through the time. The optimal size of the local regions has been determined by minimizing the local entropy dispersion. Then, the movement of each mosaic element was found by using normalized image cross-correlation between each mosaic element for the time considered and the corresponding element in the first image. To improve the accuracy of the measurement, a thin-plate splines interpolation was applied on the neighborhood of the correlation peak.

The first noticeable result is that inefficient use of the luminance dynamic range decreases the expected accuracy of the method. This was already pointed out by the authors in [16] but we have demonstrated here the practical implications of this problem. It is worth to mention that, although in this experiment this problem appears in a region of the image, the final result will affect to the whole image, since results are combined in order to obtain the compression and dilation of the piece.

Our results show that we are able to determine the local concrete deformation with reasonable accuracy even without the use of a painted pattern. Even accounting that the results of a camera are worse than those obtained with a strain gauge, the importance of our proposal relays in the possibility of measuring inaccessible structures or historical buildings where it is complicated or even impossible to paint a uniform speckle pattern in the surface. The adjustment of the

procedure to the particular quality and grain distribution of the image gives an additional advantage to the ad hoc implementation. Despite the experiment was implemented inside a lab, the conditions used are close to which can be found in the measurement of a real structure at its emplacement.

REFERENCES

[1] Bing Pan, Dafang Wu, Zhaoyang Wang "Internal displacement and strain measurement using digital volume correlation: a least-squares framework" Measurement science and Technology, 23, 045002 (13pp) (2012)

[2] Bing Pan, Huimin Xie, Zhaoyang Wang, Kemao Qian, Zhiyong Wang "Study on subset size selection in digital image correlation for speckel patterns" Optic Express, 16 (10) pp. 7037-7048 (2008)

[3] M. A. Sutton, J. Orteu, H. Schreier, *Image Correlation for Shape, Motion and Deformation Measurements,* SpringerLink (2009).

[4] Chris A. Murray, Neil A. Hoult, W. Andy Take "Dynamic measurement using digital image correlation" International Journal of Physical Modelling in Geothecnics", 17 (1) pp. 41-52 (2016)

[5] White D. J., Take W. A. "GeoPIV: Particle Image Velocimetry (PIV) software for use in geotechnical testing" Cambridge University Engineering Department, Technical report CUED/D-SOILS/TR322 (2002)

[6] S. A. Stainer, J. Blaber, W. A. Take, D. J. White "Improved image-based deformation measurement for geotechnical applications" Canadian Geotechnical Journal 53, pp. 727-739 (2016)

[7] J. Blaber, B. Adair, A. Antoniou, "Ncorr: Open-source 2D digital image correlation Matlab software" Experimental Mechanics, 15 (6) pp. 1105-1122 (2015)

[8] www.gom-correlate.com , last time accessed on August 2017

[9] S. Y. Alam, A. Loukili, F. Grondin, E. Rozière "Use of the digital image correlation and acoustic emission technique to study the effect of structural size on cracking of reinforced concrete" Engineering fracture mechanics 143, pp. 17-31 (2015)

[10] Hyunjun kim, Eunjong Ahn, Soojin Cho, Myoungsu Shin, Sung-Han Sim "Comparative analysis of image binarization methods for crack identification in concrete structures" Cement and concrete research 99, pp. 53-61 (2017)

[11] H. Mammand, J. Chen, "Extended digital image correlation method for mapping multiscale damage in concrete" Journal of materials in civil engineering, 29 (10): 04017179 (2017)

[12] A. Acciaioli, G. Lionello, M. Baleani, “Experimentally achievable accuracy using a digital image correlation technique in measuring small-magnitude (<0.1%) homogeneous strain fields” Materials, 11(751), ma11050751 (2018)

[13], R. C. Gonzalez, R. E. Woods, S. L Eddins *Digital image processing using MATLAB* (chapter 11), New Jersey, Prentice Hall (2003)ç

[14] Thin-plate spline, *Wikipedia (last seen in May, 2018)*. https://en.wikipedia.org/wiki/Thin_plate_spline

[15] D. Michaelis, D. R. Neal, B. Wieneke “Peak-locking reduction for particle image velocimetry*” Measurement Science and Technology* 27, nr. 104005 (2016)

[16] D. Mas, J. Perez, B. Ferrer, J Espinosa. “Realistic limits for subpixel movement detection”. *Applied Optics 55,* 4974-4979 (2016)